

On the “hidden” harmonics associated to best approximants due to quasi-periodicity in splitting phenomena

E. Fontich, C. Simó, A. Viero
Departament de Matemàtiques i Informàtica
Universitat de Barcelona
BGSMath
Gran Via, 585, 08007, Barcelona, Catalonia

September 9, 2018

Abstract

The effects of quasi-periodicity on the splitting of invariant manifolds are examined. We have found that some harmonics, that could be expected to be dominant in some ranges of the perturbation parameter, actually are non-dominant. It is proved that, under reasonable conditions, this is due to the arithmetic properties of the frequencies.

Keywords: quasi-periodic splitting, dominant harmonics, hidden harmonics, irrational numbers properties

MSC: 37C55, 37J40, 37J45

Remembering Jürgen Moser 90 years after his birth

1 Introduction

Jürgen Moser, one of the greatest mathematicians of the XXth century, did a lot of works concerning quasi-periodic aspects of the dynamics. Beyond the persistence of invariant curves in perturbations of integrable area-preserving maps [13] (equivalent to persistence of tori in some Hamiltonian systems), when the frequency on the curves satisfies suitable Diophantine conditions, a non-degeneracy condition is satisfied and the perturbation is small enough, he produced a huge amount of papers, books and contributions to books concerning many other aspects of quasi-periodic phenomena. See, e.g., [14].

In this paper we deal with a related problem. We study the splitting of separatrices of a periodically perturbed integrable system that depends on a small parameter, say ν , for which, due to a combination of a frequency of the integrable problem and the one of the periodic perturbation, the splitting shows quasi-periodicity.

In [9] one has considered as model a Hamiltonian-Hopf bifurcation of a fixed point, that we assume located at the origin, in a Hamiltonian system of two degrees of freedom. As it is well known, before the bifurcation the point is totally elliptic with eigenvalues $\pm\omega_1 i, \pm\omega_2 i$ being ω_1 and ω_2 rather close. Then, at the bifurcation the eigenvalues become $\pm\omega_c i$ double and after the bifurcation the system has a complex-saddle fixed point at the origin, which eigenvalues $\pm\nu \pm \omega i$, being ω close to ω_c and $\nu > 0$ small. Using the Sokolskii normal form around the fixed point, truncated at order four and with suitable sign of the four order terms, its stable and unstable manifolds are compact and coincide, the homoclinic solutions tend to the fixed point as $\text{sech}(\nu t)$ and have periodic factors with frequency close to ω_c . After a suitable normalization we can consider that these factors have unit frequency. Then the effects of a perturbation with a factor which depends periodically on time with frequency γ are studied. See Sect. 2 for a

summary on this model and Sect. 3 for a sample of results. In the present study the parameters which appear in the perturbation are kept constant. The relevant small parameter will be the real part ν of the eigenvalue at the origin. See [9] for changes associated to some variations of the parameters which appear in the perturbation.

A Hamiltonian-Hopf bifurcation appears in problems related to physical phenomena. As a recent example we refer to [15] where the problem of the dynamics of the hydrogen atom in a circularly polarized microwave field is shown to display such bifurcation. For a detailed description of the behavior of the electron and simulations of the phase space structure see [1].

It is well known that if only one angle plays a role and its frequency is fixed, say equal to 1 after suitable scaling, the splitting depends on one angle and the amplitude is, generically, of the order of $\exp(-c/\nu)$. This is clearly an averaging effect. But in the quasi-periodic case, if beyond that frequency there is another one equal to $\gamma \notin \mathbb{Q}$, then combinations like $k_1 + k_2\gamma$, $k_1, k_2 \in \mathbb{Z}$, appear as frequencies. They can be small, specially if (k_1, k_2) is selected as $(N_k, -D_k)$ where N_k/D_k is a best approximant (BA) of γ . In such case the averaging effect is worse [18] and one can expect an splitting amplitude of the order of $\exp(-c/\sqrt{\nu})$ or similar. See again [9] and Appendix B in particular.

It is reasonable to expect that the harmonics associated to best approximants of γ (HBA for short) give the largest contributions to the splitting. But this depends on the amplitudes of the related coefficients. If they are zero or very small, the contribution will be negligible. Hence, one can make assumptions on the rate of decay of the coefficients of the harmonics which appear in the perturbation. In Sect. 4 we take into account this fact and assume an exponential decay, say of the form $\exp(-|k_1|\rho_1 - |k_2|\rho_2)$, $\rho_1 > 0, \rho_2 > 0$, for the harmonic with frequency $k_1 + k_2\gamma$. See also Remark 5.2. at the end of Sect. 5 for comments on other cases.

The HBA are expected to be the dominant harmonics for some ranges of ν . One can question if there are HBA which are never the dominant ones. One can say that they are “hidden”. This has been observed in [9] for some of the considered values of γ . The main goal of the present work is to characterize the presence of hidden HBA and how this depends on the arithmetic properties of γ . The results concerning this topic are in Sect. 5.

The values of γ considered in Sect. 3 are either quadratic irrationals or numbers whose continued fraction expansion (CFE) has very special properties. These CFE do not satisfy some of the “typical” properties which appear for sets of irrational numbers of full measure. In Sect. 6 we consider several examples (chosen in a rather arbitrary way), we check that there is a strong numerical evidence that they satisfy these typical properties and then we look at some curious property concerning the distribution of hidden HBA.

The same kind of phenomena appears in another context in many papers, related to the exponentially small splitting of the invariant manifolds of whiskered tori in any dimension. The existence of the splitting was studied in detail in [16] and the results were summarized in [17], where different values of the ratio of frequencies γ are studied numerically in some examples. The first three examples concern values of γ of constant type (the quotients in the CFE are bounded). Last example is not of constant type, but it satisfies a bound of the form $|p - q\gamma| > c \log(\log(q))/(q \log(q))$ for $c > 0$ and all $q \geq 3$ (see Lemma 7.3 in [9] for a proof). For cases in which one considers also the existence of resonant frequencies in the ones which appear in the splitting of whiskered tori we refer to [12]. Several other papers are concerned with the splitting, transversality and continuation of transverse homoclinic orbits, using different types of frequency ratios (see [6, 7, 3, 4, 5]). The numerical simulations which appear in some of these papers show also evidences of the existence of hidden HBA.

Before ending the Introduction we should add some comments on the fact that the exponentially small character is due to averaging properties. In [18] one considers the averaging of fast quasi-periodic forcing in a general setting, giving rough upper bounds, looking at the effects on

a perturbed pendulum and presenting numerical examples showing the changes on the dominant harmonics which show up. A careful theoretical study with good estimates appears in [8]. In [19] one considers the effect of the splitting in the classical Arnold's example of diffusion with two equal parameters. The reader can ask why a term with frequency $N_k - \gamma D_k$, where N_k/D_k is a best approximant of γ should be considered as a "fast" frequency because, in fact, it can be very small. The reason is that in the present problem the rate of increase of the distance from the fixed point behaves rather slowly, as $\exp(\nu t)$. If one changes time to a new time $\hat{t} = \nu t$ the rate is the usual exponential. But the change of the time scale means that the "slow" frequencies should be multiplied by $1/\nu$. According to the results in Section 4, trying to minimize (9), for the approximant N_k/D_k which becomes dominant for a given value of ν , it turns out that the scaled frequency is of the order of $\nu^{-1/2}$ in the case of constant type γ and can be larger in the other cases. So, they can be considered as "fast" frequencies.

2 The model and a first perturbation

Consider a Hamiltonian-Hopf bifurcation which is produced at a fixed point, located at the origin, of a Hamiltonian with two degrees of freedom. When the fixed point is of complex-saddle type, keeping terms in the normal form up to degree 4, selecting the sign of the terms of degree 4 so that the invariant manifolds of the origin become bounded, and scaling in a suitable way, one has the integrable Hamiltonian

$$H_0(x_1, x_2, y_1, y_2) = \Gamma_1 + \nu(\Gamma_2 - \Gamma_3 + \Gamma_3^2), \quad (1)$$

where $\nu > 0$, $\Gamma_1 = x_1 y_2 - x_2 y_1$, $\Gamma_2 = (x_1^2 + x_2^2)/2$ and $\Gamma_3 = (y_1^2 + y_2^2)/2$. The functions $G_1 = \Gamma_1$ and $G_2 = \Gamma_2 - \Gamma_3 + \Gamma_3^2$ are first integrals of the system, functionally independent almost everywhere and in involution. They are equal to zero along the invariant manifolds of the origin for H_0 . In this paper we shall consider the variations of G_1 along the manifolds, due to a perturbation. The variations of G_2 are quite similar, see [9]. We recall that the eigenvalues at the origin are $\pm\nu \pm i$.

The invariant manifolds $W^{u/s}(\mathbf{0})$ are given by $\{H_0 = 0\} \cap \{\Gamma_1 = 0\}$. They are foliated by homoclinic orbits $\Phi_{\psi_0}(t) = (x_1(t), x_2(t), y_1(t), y_2(t))$ given by

$$x_1(t) = -R_1(t) \cos(\psi), \quad x_2(t) = -R_1(t) \sin(\psi), \quad y_1(t) = R_2(t) \cos(\psi), \quad y_2(t) = R_2(t) \sin(\psi), \quad (2)$$

being $\psi = t + \psi_0$, $R_1(t) = \sqrt{2} \operatorname{sech}(\nu t) \tanh(\nu t)$, and $R_2(t) = \sqrt{2} \operatorname{sech}(\nu t)$. The value of ψ_0 is an initial phase. In particular, $\Phi_{\psi_0}(t)$ has singularities at $t = (2n + 1)i\pi/2\nu$, $n \in \mathbb{Z}$. See [9] for details. In particular, if we restrict the attention to the R_1 and R_2 variables, one recovers the well known separatrix of Duffing's model.

Then, following again [9], one adds a perturbation εH_1 of the form

$$H_1(x_1, x_2, y_1, y_2, t) = g(y_1)f(\theta), \quad g(y_1) = \frac{y_1^5}{d - y_1}, \quad f(\theta) = \frac{1}{c - \cos(\theta)}, \quad \theta = \gamma t + \theta_0, \quad (3)$$

where θ_0 is a phase. This choice of H_1 keeps the terms up to order four in $H = H_0 + \varepsilon H_1$ unchanged. In particular the fixed point of the perturbed problem is still the origin. We note that, when evaluated along the unperturbed homoclinic orbits, H_1 contains harmonics with argument $k_1\psi + k_2\theta$ for all the values of k_1 and k_2 . For concreteness one has used fixed values $d = 7$, $c = 5$ and $\varepsilon = 10^{-3}$ and then ν is considered as the perturbative small parameter. We shall mention later the values of γ that have been used. The expressions in (3) show that in the Taylor (resp. Fourier) expansion of g (resp. f) one passes from one term to the next one by dividing the coefficient by d (resp. by $\rho_c = c + \sqrt{c^2 - 1}$).

The perturbation produces changes in $W^{u/s}(\mathbf{0})$ leading to splitting: the manifolds do not longer coincide. For concreteness we look at the splitting in a Poincaré section, Σ . It is convenient

to define Σ as the place where R_2 reaches a maximum or, equivalently, where $R_2^2 = y_1^2 + y_2^2$ reaches a maximum. In the unperturbed case this would be $R_2 = \sqrt{2}$. In the parametrization given for R_2 this corresponds to $t = 0$. The intersection of $W^u(\mathbf{0})$ with Σ can be seen as a graph on a 2D torus where the angles correspond to two phases $\psi_1, \theta_1 \in [0, 2\pi)$, which are the values of ψ, θ for a point in $W^u(\mathbf{0})$ when it reaches Σ . The same happens for $W^s(\mathbf{0})$. The splitting is given by the difference of the functions describing the graphs.

For simplicity we present here the splitting effect produced in the first integral Γ_1 . A similar method can be used for any other independent first integral, see [9]. To compute the splitting two different approaches have been considered:

1. **A numerical approach.** We begin with $W^u(\mathbf{0})$ for the perturbed problem. One starts at a local approximation near the origin with values of the initial phases $\psi_0, \theta_0 \in [0, 2\pi)$ in an equispaced lattice (in practice we use 512×512 points). Then the equations of motion are integrated using a high order Taylor method until the solutions reach Σ .

To have a nice representation of the values of Γ_1 when we reach Σ , say \tilde{F}_1^u , we would like to have values of ψ, θ , to be denoted as ψ_1, θ_1 , also in an equispaced lattice. This is achieved using Newton method.

In this way \tilde{F}_1^u is seen as a graph in Σ . A similar thing is done for $W^s(\mathbf{0})$, getting the intersection with Σ as the graph of \tilde{F}_1^s . The splitting is given by $\Delta\tilde{F}_1 = \tilde{F}_1^u - \tilde{F}_1^s$.

2. **An analytic approach.** To this end we use the first order variational equation wrt ε , that is the first order Poincaré-Melnikov method. This first order splitting is given by

$$\Delta F_1^{(1)} = \varepsilon \int_{-\infty}^{\infty} \{\Gamma_1, H_1\} \circ \Phi(s) ds, \quad (4)$$

where we recall that Φ denotes the homoclinic solutions for H_0 . Due to the shape of the perturbation one has in (4) that $\{\Gamma_1, H_1\} = y_2 \frac{dg}{dy_1}(y_1) f(\theta)$. To be able to compare with $\Delta\tilde{F}_1$, the initial phases in the angle ψ in Φ and in the angle θ are taken equal to ψ_1 and θ_1 , respectively.

Due to the powers of $\cos(\psi)$ and $\cos(\theta)$ which appear in H_1 (and also the term in $\sin(\psi)$ due to y_2) the integral in (4) contains harmonics of the form $\sin(k_1\psi_1 - k_2\theta_1)$, for arbitrary integer values of k_1 and k_2 , with numerical factors F_{k_1, k_2} that follow from the integrals. The fact that no terms in $\cos(k_1\psi_1 - k_2\theta_1)$ appear is due to the parities of the functions in $\{\Gamma_1, H_1\}$. These numerical factors involve the integrals $I_1(s, \nu, n) = \int_{\mathbb{R}} \frac{\cos(st)}{(\cosh(\nu t))^n} dt$, where $n \geq 1, s = k_1 - k_2\gamma$, and factors decreasing as negative powers of d and ρ_c . See [9] for analytic expressions for $I_1(s, \nu, n)$ and the explicit sums that give the value of $\Delta F_1^{(1)}$.

In the argument of the harmonics, $k_1\psi_1 - k_2\theta_1$, it is not restrictive to assume $k_1 > 0$. Also the harmonics that will be more interesting should have $k_2 > 0$ for small values of ν . The reason is that the associated frequencies in the computation of $\Delta F_1^{(1)}$ should be (relatively) small. Large frequencies average very well and they have small contributions to the splitting. Even more, as it will be discussed in Sect. 5 the relevant contributions come from k_1 and k_2 such that k_1/k_2 is a best approximant of γ .

To have a feeling about how $W^u(\mathbf{0})$ change under the effect of the perturbation one should recur to a high dimensional plot, because of the 4 variables and the effect of time. The manifolds are three-dimensional, one variable measuring the distance to the origin near the fixed point and the two angles ψ, θ . A simpler way could be to plot the projection on the (x_1, y_1) variables when $x_2(t) = 0$. With the parameters d, c and ε used for the perturbation, the plot is extremely close to the manifolds of Duffing's problem. It can be checked in several figures in [9] that, even for relatively large values of ν (e.g. $\nu = 1/16$) the difference with the figure eight Duffing's manifolds is below 10^{-3} .

3 A sample of results

Initially we have restricted the study of the splitting to the value of γ equal to the golden mean $(\sqrt{5} - 1)/2$.

The results obtained using both approaches in Sect. 2 have been compared for values of ν not too small (i.e., for $\nu \geq 2^{-7}$) using values with step 0.005 in \log_2 scale. For the numerical approach quadruple precision has been used and this range is feasible in a reasonable CPU time.

It is relevant to remark that, concerning the analytical approach for a concrete value of ν , there are infinitely many terms in the Poincaré-Melnikov expressions. One has selected harmonics such that their contribution is larger than 10^{-10} times the largest contribution. For values of $\nu < 10^{-3}$ at most three harmonics satisfy this criterion (for values of the order of 0.1 this number increases to 50 or more). Furthermore, in turn, every harmonic comes from infinitely many terms in $\Delta F_1^{(1)}$, but only a moderate number of them plays a role. This number can be just 1 for $\nu < 10^{-4}$. See [9] for full details.

The first evidence is that, looking at the maximal value of the splitting in the domain $\psi_1, \theta_1 \in [0, 2\pi)$, the results using both approaches are essentially coincident.

Next point of interest is what happens for smaller values of ν . Typically only one harmonic plays a role for some range of ν , then a second harmonic has also a relevant contribution when ν decreases, and a new decrease of ν implies that this second harmonic becomes dominant and the contribution of the first one is less relevant.

To illustrate this fact one has considered several values of γ : $\gamma_0, \gamma_1, \gamma_2, \gamma_3, \gamma_4$, where γ_0 is the golden mean, $\gamma_4 = e - 2$ and the other values are variants of γ_0 concerning the CFE. Concretely, the CFE used for these 5 values of γ are

$$\begin{aligned}
 \gamma_0 &= [0; 1, 1, 1, 1, 1, 1, 1, 1, 1, 1, 1, 1, 1, 1, 1, 1, \dots], \\
 \gamma_1 &= [0; 10 \times 1, 1, 10, 1, 1, 10, 1, 1, 10, 1, 1, 10, 1, 1, \dots], \\
 \gamma_2 &= [0; 10 \times 1, 1, 10, 1, 10, 1, 10, 1, 10, 1, 10, 1, 10, \dots], \\
 \gamma_3 &= [0; 10 \times 1, 2, 3, 4, 5, 6, 7, 8, 9, 10, 11, 12, 13, 14, \dots], \\
 \gamma_4 &= [0; 1, 2, 1, 1, 4, 1, 1, 6, 1, 1, 8, 1, 1, 10, 1, 1, 12, \dots],
 \end{aligned} \tag{5}$$

where 10×1 means 10 consecutive quotients equal to 1.

The Fig. 1 shows the amplitudes of the harmonics of the splitting associated to best approximants of γ (HBA), and how they evolve as a function of ν for small values of ν . This is done for the five values of γ given before. The horizontal variable in the plots is $\log_{10}(\nu)$, while the vertical variable displays the logarithm of the amplitude after a suitable scaling (see the caption). See Sect. 4 for the justifications of the scalings used in the different cases. For concreteness if the CFE of γ is $[q_0; q_1, q_2, q_3, \dots]$ the k -th approximant is denoted as $N_k/D_k = [q_0; q_1, q_2, q_3, \dots, q_k]$. The related HBA is of the form $\exp((N_k\psi_1 - D_k\theta_1)i)$.

In the plots the best approximants related to the dominant harmonic (i.e., the ones giving a larger contribution, larger vertical coordinate in the figure) going from right to left are: from 233/377 to 317811/514229 for γ_0 ; from 89/144 to 43627/70588 for γ_1 ; from 89/144 to 146794/237511 for γ_2 ; from 144/233 to 67774/109663 for γ_3 , and from 334/465 to 286565/398959 for γ_4 .

Consider two different best approximants of γ , N_k/D_k and N_l/D_l . Then the value of ν for which the amplitudes of the related HBA coincide will be denoted as $\nu_{k,l}$. We shall see later in Sect. 5 that, under suitable conditions stated in Sect. 4, this value is unique.

In the case of γ_0 we see that the maxima tend to a constant and that the differences between $\log(\nu_{k-1,k})$ and $\log(\nu_{k,k+1})$ also tend to a constant. Both things are proved in [9]. The fact that the maxima in the five cases tend to a constant when $\nu \rightarrow 0$ is due to the scalings used in the plots. For γ_1 also all the HBA dominate in some range of ν but the ones such that next

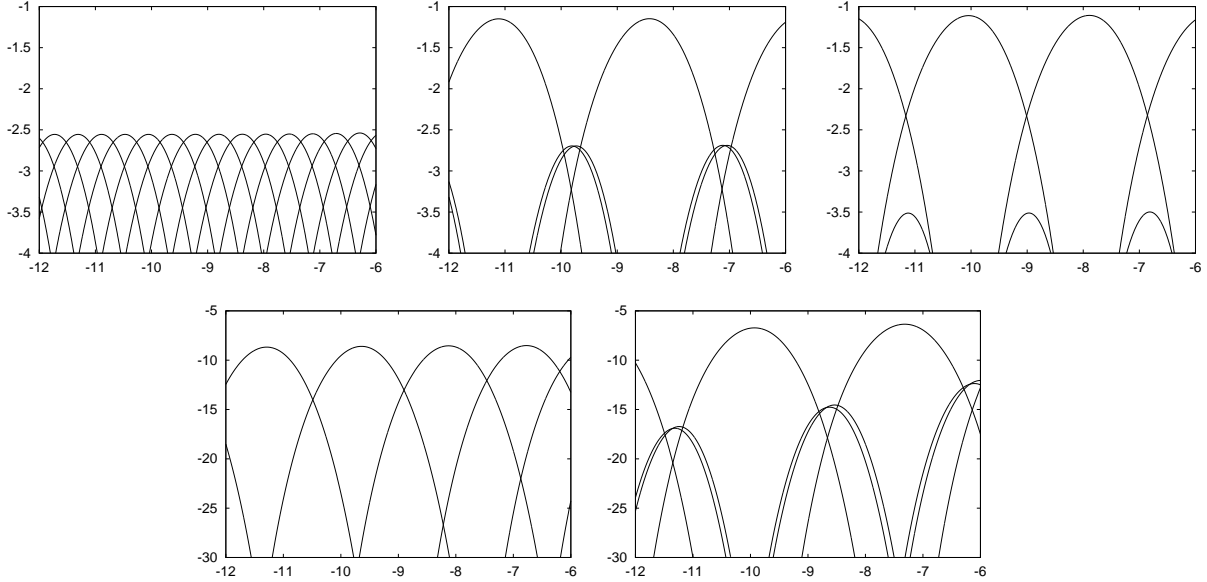


Figure 1: Plots of the contributions F_{N_k, D_k} to the splitting of harmonics associated to different best approximants, N_k/D_k , of γ . On the top row the results for γ_0, γ_1 and γ_2 are shown from left to right. On the bottom one they are shown for γ_3 and γ_4 also from left to right. The horizontal variable is $\log_{10}(\nu)$ in all the plots while the vertical variable is a scaled version of $\log(F_{N_k, D_k})$. Concretely, in the top row one plots $\sqrt{\nu} \log(|F_{N_k, D_k}|/\varepsilon)$, while in the bottom row one plots $\sqrt{\nu \log(1/\nu)} \log(|F_{N_k, D_k}|/\varepsilon)$. See the text for comments on these results and the reason for the different scalings.

quotient is $q_{k+1} = 10$ dominate in a larger range and the maxima are much higher. In contrast for γ_2 there are HBA which are never dominant. They are “hidden” and correspond to quotients $q_k = 10$ which are followed by a quotient equal to 1. For γ_3 and γ_4 all HBA dominate in a range of ν but for γ_4 , as it happens in the case of γ_1 , for some of the harmonics the range in $\log(\nu)$ is rather short. The fact that for these harmonics, which dominate in short ranks of ν , the maxima are decreasing is due to the scaling used in the plot.

Summarizing, several questions appear. Why some HBA are hidden and never dominate for any value of ν ? Which conditions should satisfy? How is this related to the quotients in the CFE of γ ? In the next section we state the assumptions to carry out the analysis and in Sect. 5 we present the results. The existence of hidden HBA was already reported in [?] in the case of a non-quadratic frequency γ of constant type.

4 Some conditions on a family of perturbations

For concreteness and to have simple representations of the coefficients of the harmonics which appear in the splitting, obtained from (4), we shall make some assumptions. They are essentially satisfied, when ν is small enough, in the case presented in sections 2 and 3. As it was considered in the model, see (3), we assume that the perturbation is a product of two functions. One of them depends on (x_1, x_2, y_1, y_2) and, therefore, when evaluated on the unperturbed homoclinic trajectories, it tends to zero when $t \rightarrow \pm\infty$ and depends periodically on ψ , see (2). The other function is periodic in θ .

- The homoclinic connections tend to zero when $t \rightarrow \pm\infty$ like the R_2 function before, i.e., like $\text{sech}(\nu t)$ or similar.
- The part of the perturbation which depends on the angle ψ appearing in the homoclinic connections, say $\mathcal{P}_1(t, \psi)$, is of the form $\sum_{j \geq 1} A_j(t) \sin(j\psi)$, with $\psi = t + \psi_1$, and the

coefficients A_j depend on powers of $\operatorname{sech}(\nu t)$ and $\|A_j\|$ behaves as $\exp(-j\rho_1)$, for t real, with $\rho_1 > 0$.

- The periodic part of the perturbation which depends on the angle θ and has frequency γ , say $\mathcal{P}_2(\theta)$, is of the form $B \sum_{j \geq 1} \exp(-j\rho_2) \cos(j\theta)$, $B \in \mathbb{R}$, with $\theta = \gamma t + \theta_1$ and $\rho_2 > 0$.

Then the contribution to (4) which appears multiplying $\sin(k_1\psi_1 - k_2\theta_1)$ requires, essentially, to evaluate terms of the form

$$\varepsilon C \exp(-k_1\rho_1 - k_2\rho_2) I_1(s, \nu, n), \quad I_1(s, \nu, n) = \int_{-\infty}^{\infty} \frac{\cos(st)}{(\cosh(\nu t))^n} dt, \quad (6)$$

where $s = |k_1 - k_2\gamma|$, C contains the factor B and some combinatorial numbers depending on k_1, k_2 . Other terms cancel because the integrand is odd or can be neglected because the related frequency is $k_1 + k_2\gamma$ and averages much better. The integrals $I_1(s, \nu, n)$ can be obtained from $I_1(s, \nu, 1) = (\pi/\nu) \operatorname{sech}(s\pi/(2\nu))$ and $I_1(s, \nu, 2) = (s\pi/\nu^2) \operatorname{cosech}(s\pi/(2\nu))$ by recurrence.

Taking logarithms in (6) and neglecting the contribution of $\log(\nu)$, $\log(k_i)$, $i = 1, 2$, of constant terms and terms relatively exponentially small in ν in front of dominant terms, one can assume that the largest contributions to the logarithm of the expression (4) are of the form

$$-k_1\rho_1 - k_2\rho_2 - \frac{s\pi}{2\nu}. \quad (7)$$

Being interested in the largest values of (7) it is advisable to take k_1/k_2 as a best approximant N_k/D_k of γ , to minimize s . Furthermore, N_k in front of ρ_1 can be approximated by γD_k with negligible errors $\mathcal{O}(D_k^{-1})$. We can replace $-N_k\rho_1 - D_k\rho_2$ by $-D_k(\gamma\rho_1 + \rho_2)$. For simplicity we introduce $\hat{\nu} = 2\nu(\gamma\rho_1 + \rho_2)/\pi$ and, immediately, we rename $\hat{\nu}$ as ν again. Finally we recall that s can be expressed, using CFE, as

$$s_k = \frac{1}{D_k c_k}, \quad c_k = c_k^+ + \frac{1}{c_k^-}, \quad c_k^+ = [q_{k+1}; q_{k+2}, q_{k+3}, \dots], \quad c_k^- = [q_k; q_{k-1}, q_{k-2}, \dots, q_1] \quad (8)$$

(see [9] for details). In particular this shows that a large value of q_{k+1} implies that N_k/D_k is a very good approximant of γ .

Hence, we are interested in minimizing

$$T(\nu, D_k) = D_k + \frac{s_k}{\nu} = D_k + \frac{1}{\nu D_k c_k}. \quad (9)$$

Given a value of ν the approximate value of D_k minimizing $T(\nu, D_k)$, and therefore giving the largest amplitude of the contribution to the splitting of this HBA, depends on the arithmetic properties of γ .

From the expression of c_k one has $q_{k+1} < c_k < q_{k+1} + 2$. Let us consider several cases for γ . If it satisfies $|p - q\gamma| \geq c/q^\tau$, for some $\tau \geq 1, c > 0$ and for all $q > 0, p \in \mathbb{Z}$ (a typical Diophantine condition, including the constant type numbers when $\tau = 1$) then a bound of $T(\nu, D_k)$ is $\mathcal{O}(1/\nu^{1/(\tau+1)})$ in agreement with the upper bounds in [18]. Note that in that case one has $q_{k+1} = \mathcal{O}(D_k^{\tau-1})$. The plots on the top row of Fig. 1 are examples for which $\tau = 1$. This is what suggests to scale multiplying by $\sqrt{\nu}$.

We can consider another type of condition, like $|p - q\gamma| \geq c/(q(\log(q))^\sigma)$, again for some $\sigma \geq 1, c > 0$ and for all $q > 1, p \in \mathbb{Z}$. In that case a bound of $T(\nu, D_k)$ is $\mathcal{O}((\nu(\log(1/\nu))^\sigma)^{-1/2})$. This is very close to the cases in the bottom row of Fig. 1 using $\sigma = 1$. The difference is the appearance of an additional factor in $\log(\log(1/\nu))$, changing very slowly. This is what suggests to scale multiplying simply by $\sqrt{\nu \log(1/\nu)}$.

We remark that the set of irrational numbers which satisfy the mentioned conditions, either $|p - q\gamma| \geq c/q^\tau$, with $\tau > 1$, or $|p - q\gamma| \geq c/(q(\log(q))^\sigma)$, with $\sigma > 1$, for some $c > 0$, is of full measure. See [10] for a general setting.

5 The “hidden” best approximant harmonics

To study the hidden character of some HBA we shall assume that ν is small enough and, therefore, the related denominators are large and the approximation of N_k by γD_k is sufficiently good. That is, minus the logarithm of the contribution of the best approximant N_k/D_k to the splitting, with a suitable linear scaling of ν as explained, is given by (9).

The functions $T(\nu, D_k)$, for a fixed value of D_k , are monotonically decreasing in ν . A change from the best approximant N_k/D_k to N_l/D_l , $l > k$, is produced for a value of $\nu = \nu_{k,l}$ such that $T(\nu, D_k) = T(\nu, D_l)$. This value of ν is unique and given by

$$\nu_{k,l} = \frac{s_k - s_l}{D_l - D_k}. \quad (10)$$

It is clear that the denominator is positive. To see that the value of $\nu_{k,l}$ is positive (so that for all k and $l > k$ there is a change), one must have $s_k - s_l > 0$. To prove this it is enough to show $s_k > s_{k+1}$.

Recall from (8) the expressions of s_k , c_k , c_k^+ and c_k^- . In particular one has $c_k^- = q_k + 1/c_{k-1}^-$ and $c_k^+ = q_{k+1} + 1/c_{k+1}^+$. To prove $s_k > s_{k+1}$ is equivalent to prove $D_{k+1}c_{k+1} > D_k c_k$. Using the fact that $D_{k+1} = D_k(q_{k+1} + 1/c_k^-) = D_k c_{k+1}^-$, one can divide by D_k both sides of the inequality and get that it is enough to show $c_{k+1}^- c_{k+1} > c_k$. Simple computations give

$$c_{k+1}^- c_{k+1} = c_{k+1}^- (c_{k+1}^+ + 1/c_{k+1}^-) = c_{k+1}^- c_{k+1}^+ + 1 = c_{k+1}^+ (c_{k+1}^- + 1/c_{k+1}^+), \quad (11)$$

and also

$$c_k = c_k^+ + 1/c_k^- = q_{k+1} + 1/c_{k+1}^+ + 1/c_k^- = c_{k+1}^- + 1/c_{k+1}^+. \quad (12)$$

As $c_{k+1}^+ > 1$ the inequality is proved. In particular this shows that for $k < l$ while if ν is large one has $T(\nu, D_k) < T(\nu, D_l)$, for ν approaching zero one has $T(\nu, D_k) > T(\nu, D_l)$.

Assume now that for a given value of ν the dominant HBA (that is, the one such that $T(\nu, D_k)$ is minimum) is the k -th one. As it has been just proved, all the $\nu_{k,l}$, $l > k$, are unique and positive. It can happen that $\nu_{k,k+1} < \nu_{k,k+2}$ and, therefore, when decreasing ν , the passage to dominance from the k -th HBA to the $(k+1)$ -th one, occurs after the passage from the k -th to the $(k+2)$ -th one. Hence, the $(k+1)$ -th HBA will never be dominant. It is “hidden”. Figure 2 shows two simple examples of this fact.

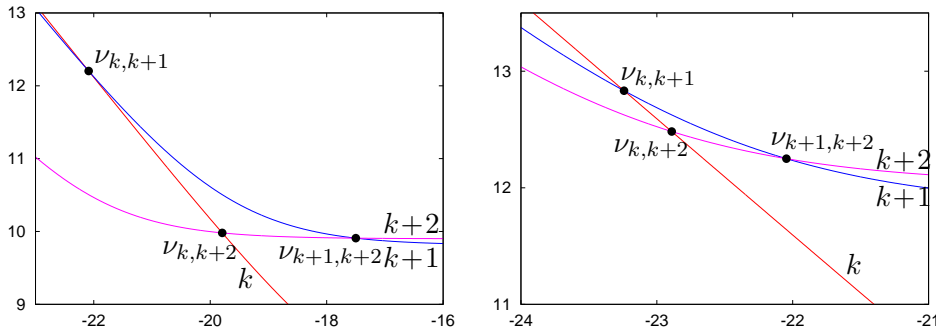


Figure 2: Plots of $\log(T(\nu, D_j))$, with T as given in (9), as a function of $\log(\nu)$ for three consecutive values of j : in red for $j=k$, in blue for $j=k+1$ and in magenta for $j=k+2$. One has $\nu_{k+1,k+2} > \nu_{k,k+2} > \nu_{k,k+1}$, corresponding to the points in black. If the k -th HBA is dominant in some range of ν starting at $\nu_{k,k+2}$ then the $(k+2)$ -th HBA is dominant in some range ending in $\nu_{k,k+2}$. The $(k+1)$ -th HBA is never dominant. The left data correspond to γ_2 (compare with the top right plot in Fig. 1), and the right one to a small modification, in order to see in a cleaner way the intersection of the blue and magenta curves, of a case which appears for $\gamma = \pi - 3$.

Now we state the main result concerning hidden HBA.

Theorem 5.1 *Assume that minus the logarithm of the amplitude of the contribution of a HBA to the splitting is given by (9) and that for some range of ν the k -th HBA is dominant. Then if the $(k+1)$ -th HBA is hidden, i.e., is not dominant for any value of ν , the following properties hold:*

1. *It is isolated, i.e., the $(k+2)$ -th HBA is not hidden. That is, no two consecutive HBA can be hidden.*
2. *The next quotient, q_{k+2} , should be equal to 1.*

Remark 5.1. We note that the change of scale of ν introduced just before (8) is not changing the order of the $\nu_{k,l}$ introduced in (10).

Proof. First we assume $q_{k+2} \geq 2$. We will prove that the $(k+1)$ -th HBA is not hidden, i.e., $\nu_{k,k+1} > \nu_{k,k+j}$, or equivalently $(s_k - s_{k+1})/(D_{k+1} - D_k) > (s_k - s_{k+j})/(D_{k+j} - D_k)$, for all $j \geq 2$. Later on we shall consider the case $q_{k+2} = 1$.

Assume $q_{k+2} \geq 2$. We will check that $D_{k+j} - D_k > 2(D_{k+1} - D_k)$ and $s_k - s_{k+j} < 2(s_k - s_{k+1})$ for $j \geq 2$. We recall that, as a function of k , D_k is strictly increasing and s_k is strictly decreasing. For the first inequality, using that $D_{k+2} = q_{k+2}D_{k+1} + D_k$, we get

$$D_{k+j} - D_k \geq D_{k+2} - D_k = q_{k+2}D_{k+1} > 2(D_{k+1} - D_k), \quad j \geq 2.$$

Since $s_{k+j} < s_k$, to prove the second inequality it is enough to check that $s_k > 2s_{k+1}$. Using $s_k = 1/(D_k c_k)$ and $D_{k+1} = D_k c_{k+1}^-$ the latter inequality is equivalent to $c_{k+1} c_{k+1}^- > 2c_k$ and, using (11) and (12), it is also equivalent to $c_{k+1}^- (c_{k+1}^+ - 2) + 1 - 2/c_{k+1}^+ > 0$. Now, this follows immediately from $c_{k+1}^+ = q_{k+2} + 1/c_{k+2}^+ > 2$.

Now we pass to the case $q_{k+2} = 1$. We plan to prove $\nu_{k,k+2} > \nu_{k,k+j}$ for all $j \geq 3$. It can happen that $\nu_{k,k+1} > \nu_{k,k+2}$, in which case the $(k+1)$ -th HBA is dominant in some range of ν or $\nu_{k,k+1} \leq \nu_{k,k+2}$ in which case the $(k+1)$ -th HBA is hidden. But only one is hidden because then the $(k+2)$ -th one is dominant. And if the $(k+1)$ -th HBA is hidden the next quotient, q_{k+2} , is equal to 1. To have $q_{k+2} = 1$ is a necessary but not sufficient condition to have the $(k+1)$ -th HBA hidden. This will complete the proof of the theorem.

To prove the inequality we shall follow a scheme similar to the case $q_{k+2} > 1$, that is, we plan to prove that $D_{k+j} - D_k \geq 2(D_{k+2} - D_k)$ and $s_k - s_{k+j} < 2(s_k - s_{k+2})$ hold for all $j \geq 3$. For the first one of these inequalities it is clear that it is enough to show $D_{k+3} - D_k \geq 2(D_{k+2} - D_k)$ and to note that the worst case appears when $q_{k+3} = 1$. In this case, from $D_{k+2} = D_{k+1} + D_k$ and $D_{k+3} = 2D_{k+1} + D_k$ one has $D_{k+3} - D_k = 2(D_{k+2} - D_k)$, as desired.

To prove $s_k - s_{k+j} < 2(s_k - s_{k+2})$ for all $j \geq 3$ it is enough to show $s_k < 2(s_k - s_{k+2})$, that is $s_k > 2s_{k+2}$, similar to what has been done if $q_{k+2} > 1$. As before, using the expressions of s_k, s_{k+2} this is equivalent to prove $2D_k c_k < D_{k+2} c_{k+2}$. To this end we express D_k and D_{k+2} as functions of D_{k+1} using c_{k+1}^- and c_{k+2}^- and we put c_k, c_{k+2} in terms of the c_*^+ and c_*^- expressions, taking into account $q_{k+2} = 1$. Concretely, after simplifying the common factor D_{k+1} , we should prove

$$2c_k/c_{k+1}^- < c_{k+2}^- (c_{k+2}^+ + 1/c_{k+2}^-) = c_{k+2}^- c_{k+2}^+ + 1.$$

For the left hand side we use

$$2c_k/c_{k+1}^- = 2(c_k^+ + 1/c_k^-)/c_{k+1}^- = 2(c_{k+1}^- + 1/c_{k+1}^+)/c_{k+1}^- = 2 + 2/(c_{k+1}^+ c_{k+1}^-).$$

Hence, we should prove

$$2/(c_{k+1}^+ c_{k+1}^-) < c_{k+2}^- c_{k+2}^+ - 1,$$

and, using the recurrence for c_{k+1}^+, c_{k+2}^- , with $q_{k+2} = 1$,

$$2c_{k+2}^+ / ((c_{k+2}^+ + 1)c_{k+1}^-) < c_{k+2}^+ (c_{k+1}^- + 1)/c_{k+1}^- - 1,$$

which can be simplified to

$$2/(c_{k+2}^+ + 1) < (c_{k+1}^- + 1) - c_{k+1}^-/c_{k+2}^+.$$

Summarizing we are led to show $c_{k+1}^-(1 - 1/c_{k+2}^+) - 2/(c_{k+2}^+ + 1) + 1 > 0$. This follows from the fact that c_{k+1}^- and c_{k+2}^+ belong to $(1, \infty)$. This finishes the proof. \square

Remark 5.2. At the beginning of Sect. 4 we assumed that the effect of the perturbation on the unperturbed invariant manifolds contains the product of two analytic functions, $\mathcal{P}_1(t, \psi)$ and $\mathcal{P}_2(\theta)$ whose Fourier coefficients decrease in an exponential way. One can question what happens if one of the functions or both of them are entire. We recall that if $\sum_{n \geq 0} \alpha_n z^n$ is entire then $-\log(|\alpha_n|)/n$ tends to ∞ when $n \rightarrow \infty$. If one of the two functions, or both of them are entire, that is, instead of the coefficients $\exp(-j\rho_1)$ and/or $\exp(-j\rho_2)$ they have a_j and/or b_j , decreasing as α_j above, the expression in (9) is replaced by a similar one

$$T^*(\nu, D_k) = D_k L_k + \frac{s_k}{\nu}.$$

The coefficient L_k comes from a combination of $-\log(|a_{N_k}|)/N_k$ and $-\log(|b_{D_k}|)/D_k$ (or of one of them and the corresponding ρ_i of the other, see (7)) and tends to ∞ as $k \rightarrow \infty$. As before we approximate N_k by γD_k . Then, for $l > k$, instead of (10) we are led to

$$\nu_{k,l}^* = \frac{s_k - s_l}{D_l L_l - D_k L_k}.$$

We want to show that the results of the theorem still hold if L_k increase in a monotone way (perhaps not strictly). For $q_{k+2} \geq 2$ the bounds $s_k - s_{k+j} < 2(s_k - s_{k+1})$, for $j > 1$, and for $q_{k+2} = 1$ the bounds $s_k - s_{k+j} < 2(s_k - s_{k+2})$, for $j > 2$, hold true as before, because they do not depend on the L_k . To show $D_{k+2}L_{k+2} - D_kL_k > 2(D_{k+1}L_{k+1} - D_kL_k)$ for $q_{k+2} \geq 2$ it is enough to use $D_{k+2}L_{k+2} \geq (2D_{k+1} + D_k)L_{k+2} > 2D_{k+1}L_{k+2} \geq 2D_{k+1}L_{k+1}$.

If $q_{k+2} = 1$ let us consider first the case $q_{k+3} \geq 2$. Then $D_{k+3} > 2D_{k+2}$ which implies $D_{k+3}L_{k+3} > 2D_{k+2}L_{k+2}$ and, hence, $D_{k+3}L_{k+3} - D_kL_k > 2(D_{k+2}L_{k+2} - D_kL_k)$.

In the remaining case, $q_{k+2} = q_{k+3} = 1$, one should proceed in a different way. Instead of $\nu_{k,k+j}^* = (s_k - s_{k+j})/(D_{k+j}L_{k+j} - D_kL_k)$ one can use, for the comparisons, the expressions $\hat{\nu}_{k,k+j} = (s_k - s_{k+j})/D_{k+j}$. Indeed, the bounds $\hat{\nu}_{k,k+j_1} > \hat{\nu}_{k,k+j_2}$ imply $\nu_{k,k+j_1}^* > \nu_{k,k+j_2}^*$.

Concretely, it is enough to show that $\max\{\hat{\nu}_{k,k+1}, \hat{\nu}_{k,k+2}\} > \hat{\nu}_{k,k+3}$. To this end we note that, using $q_{k+2} = q_{k+3} = 1$, all the terms in the last inequality can be expressed as simple functions of $D_k, q_{k+1} \in \mathbb{N}_+, c_{k+3}^+ > 1$ and $c_k^- > 1$. Both $\hat{\nu}_{k,k+1} - \hat{\nu}_{k,k+3}$ and $\hat{\nu}_{k,k+2} - \hat{\nu}_{k,k+3}$ become simple rational expressions in q_{k+1}, c_{k+3}^+ and c_k^- with a common factor D_k^{-2} . One has $\hat{\nu}_{k,k+1} - \hat{\nu}_{k,k+3} > 0$ in all cases and also $\hat{\nu}_{k,k+2} - \hat{\nu}_{k,k+1} > 0$ if $c_{k+3}^+ < q_{k+1} + 1/c_k^-$. That is, if the k -th HBA is not hidden, either the $(k+1)$ -th or the $(k+2)$ -th one are not hidden, and if one of them is hidden the next quotient is equal to 1.

This ends the proof of the validity of the theorem in the entire case if L_k is increasing.

However we note that it is very easy to produce examples in which the results are not true in the entire case if, despite L_k tends to ∞ , there are ranges in which L_k decreases. Concretely, assume the k -th HBA is not hidden and, given $j \geq 3$, consider values $L_{k+1}, \dots, L_{k+j-1}$ which are identical or increase slowly. Then assume L_{k+j} smaller, such that $D_{k+j}L_{k+j} - D_kL_k$ is positive but rather small. The next dominant HBA after the k -th one will be the $(k+j)$ -th one, and $j-1$ consecutive HBA will be hidden.

6 On the behavior of some transcendental numbers

In Sect. 3 we have looked at the behavior of the HBA for the values $\gamma_j, j = 0, \dots, 4$. The results were illustrated in Fig. 1. Only in the case of γ_2 there appear hidden HBA. But it is clear that

the CFE of these values of γ are quite exceptional. Hence, it seems natural to look for what happens for “typical” $\gamma \in (0, 1), \gamma \notin \mathbb{Q}$.

This leads to the question about what means “typical”. One can assume that a number γ is typical if it satisfies properties which hold for a set of numbers of full measure. Let us recall a couple of them (see [10] for details).

- The geometric mean of the quotients of the CFE tends to the so-called Khinchin constant $KC \approx 2.6854520010653064$ (see, e.g., <https://oeis.org/A002210> for more digits) or, equivalently, the arithmetic mean of the logarithms of the quotients tends to $\log(KC) \approx 0.9878490568338104$.
- The rate of increase of the denominators of the best approximants N_k/D_k of γ satisfies $\lim_{n \rightarrow \infty} \log(D_n)/n \rightarrow LC$, the Lévy constant, $LC = \pi^2/(12 \log(2)) \approx 1.1865691104156255$. Equivalently, the denominators tend to behave as $D_k \approx (\exp(LC))^k$, where $\exp(LC) \approx 3.2758229187218112$.

Another property follows from the fact that the Gauss map in $(0, 1) : x \mapsto 1/x - E[1/x]$, where $E[\cdot]$ denotes the integer part, has $(1+x)^{-1}/\log(2)$ as ergodic invariant measure, see [11]. This gives that the probability to have k as quotient is $P(k) = \log_2(1 + 1/(k^2 + 2k))$, the Gauss-Kuzmin law.

It is important to remark, from this law, that the apparition of the different quotients is not random: the successive events are not independent. As a first example, the probability of having 1 as quotient is $P(1) = \log_2(4/3)$. But the probability of having two consecutive quotients equal to 1 is $P(1, 1) = \log_2(10/9)$ and one has $P(1, 1) < P(1)^2$. In general, the probability to have k and l as consecutive quotients (or vice versa) is $P(k, l) = \log_2(1 + 1/(((k+1)l+1)((l+1)k+1)))$. One has $P(k, l) > P(k)P(l)$ only if $k = 1, l > 2$ or if $k = 2$ and $2 \leq l \leq 5$ (or if the roles of k and l are exchanged), as it is easy to prove. In all other cases one has the converse inequality. This is independent of how many quotients appear before the couple (k, l) . It is immediate to obtain the expression for $P(k, l)$ if they are the first two quotients. But if they appear after m previous quotients, the set of numbers having k and l as the $(m+1)$ -th and $(m+2)$ -th quotients is the m -th preimage under the Gauss map of the set in which they appear as the first ones.

Note also that if one generates successive quotients with the Gauss-Kuzmin law in an independent way, Khinchin property will be satisfied, but Lévy one will not be guaranteed.

To do some tests we have chosen, in a completely arbitrary way, 6 values of $\gamma : \gamma_j^* \in (0, 1), j = 1, \dots, 6$, as follows:

$$\gamma_1^* = \pi - 3, \gamma_2^* = \exp(g) - 1, \gamma_3^* = \exp(\sqrt{2}) - 4, \gamma_4^* = \exp(\sqrt{3}) - 5, \gamma_5^* = \exp(\sqrt{5}) - 9, \gamma_6^* = \exp(\sqrt{7}) - 14, \tag{13}$$

where $g = (\sqrt{5} - 1)/2$, the golden number. Different aspects have been considered. For all of them, to proceed with the required accuracy, one has used the package [2].

- We have looked for the initial quotients of the CFE for the $\gamma_j^*, j = 1, \dots, 6$. Assume that we compute n quotients. Let $P^*(k)$ be the fraction of quotients equal to k while $P(k)$ is the theoretical value. From this one can compute the cumulative distribution function $CDF(k) = \sum_{j=1}^k P(k)$ and, in a similar way, we compute $CDF^*(k)$ for a given γ_j^* . To compare both CDF we use the Kolmogorov-Smirnov test $KS = \max_k |CDF^*(k) - CDF(k)|$. If $n = 10^7$ and consider just quotients up to $q_k = 10^4$, the maximum of the values of KS for $\gamma_j^*, j = 1, \dots, 6$ is 0.00028. Using $n = 5 \times 10^7$ for γ_1^* and γ_2^* (and again $q_k \leq 10^4$) the maximum is 0.00009. These are very small values to pass the KS test.
- As an additional check we compute the autocorrelation of the quotients. Given the quotients q_1, \dots, q_k, \dots we look for the correlation when the indices have been shifted by m

units, $m = 1, 2, 3, \dots$. As it can be expected from the lack of independence of the events, there is some autocorrelation. The autocorrelation has been computed up to $m = 1000$ and the results are shown, for all the γ_j^* together, in Fig. 3, left.

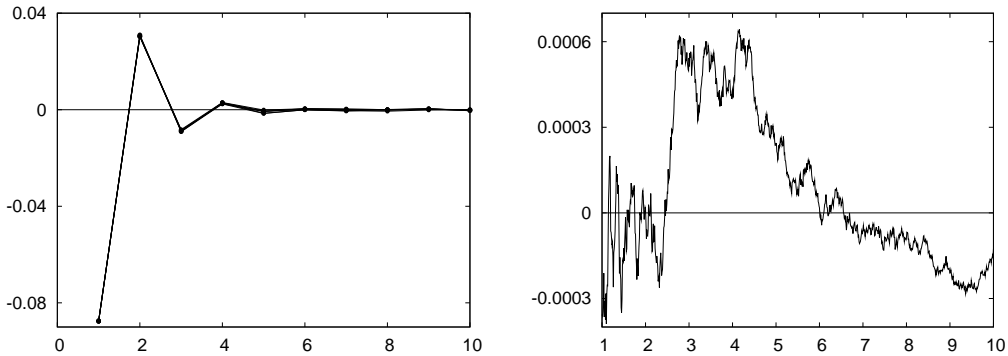


Figure 3: Left: Plots of autocorrelation coefficient ρ as a function of the shift, m , of the indices. All the γ_j^* are displayed and almost coincide. For $m \geq 6$ the values satisfy $|\rho| < 0.0013$ for all the γ_j^* . Right: Differences between $\log(D_n)/n$ and LC for γ_5^* and n between 10^6 and 10^7 , plotted with step 10^4 in n . The horizontal variable is $n/10^6$. See the text for more information.

- Now we comment on the experimental tests related to Khinchin and Lévy constants. After computing n quotients and denominators one can check the behavior of the ratios $R_{KC}(n) := (\sum_{k=1}^n \log(q_k))/n$ and $R_{LC}(n) := \log(D_n)/n$, both as functions of n . The Fig. 3, right, shows the evolution of $R_{LC}(n)$ for $10^6 \leq n \leq 10^7$ for γ_5^* . The evolution for $R_{KC}(n)$ is similar. With small variants (larger differences wrt the expected limit for some n , smaller for other) similar things happen for the other γ_j^* . Furthermore, it has been checked that for $45 \times 10^6 \leq n \leq 50 \times 10^6$ the differences $|R_{KC}(n) - \log(KC)|$ and $|R_{LC}(n) - LC|$ are less than 0.000298 for γ_1^* and even less than 0.000048 for γ_2^* . All this gives good evidence that the γ_j^* seem to be in agreement with the expected Khinchin and Lévy limits.
- Another item is which kind of Diophantine condition is satisfied by a given γ . As discussed in Sect. 4 when considering the scalings, we can check if these frequencies satisfy a condition of the form $|N_k - \gamma D_k| = (D_k c_k)^{-1} > c/(D_k (\log(D_k))^\sigma)$ for $c > 0, \sigma > 1$. We report on some results for $\gamma_1^* = \pi - 3$. For the other γ_j^* there are similar results.

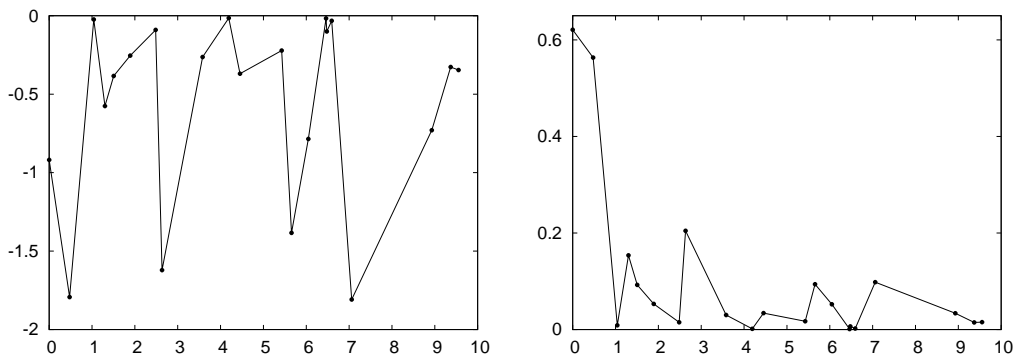


Figure 4: Results displayed for γ_1^* . Left: Values of $\Delta_k := s_k D_k \log(D_k)$ as a function of k , using \log_{10} scale for both variables, plotting only the values of k such that $\Delta_k < 1$. Right: For the same values of k we display σ to have $s_k = 1/(D_k (\log(D_k))^\sigma)$, that is, asking for $c = 1$. The plot is also in \log_{10} scale for both variables.

To fix ideas we assume $c = 1$ and then compute σ . One could reduce σ at the price of taking c rather small, not convenient for small divisors estimates. From the data computed for γ_1^* we look first to the indices $k < 2 \times 10^7$ such that $\Delta_k := s_k D_k \log(D_k)$ is less than 1. These will be the ones which require $\sigma > 1$. The data that we compute are complemented with data provided by Eric W. Weisstein (see <https://oeis.org/A033089> and <https://oeis.org/A033090>) based on the computation of the first 15×10^9 quotients of the CFE of π , which give k and q_k for large q_k . From these data, using q_k to estimate c_{k-1} and $\log(D_{k-1}) \approx LC \times (k-1)$, one can compute the related values of σ . But they play a small role. The results are shown in Fig. 4.

The large values of σ for $k = 1$ and $k = 3$ (≈ 4.177771 and ≈ 3.657928 , respectively), which are seen in the right plot, are due to the “classical” approximations of π : $22/7$ and $355/113$. Letting them aside the worst case appears for $k = 430$, with $q_{431} = 20776$, and gives $\sigma \approx 1.601339$. This value can be used up to $k^* = 15 \times 10^9$, excluding the “classical” approximants. We also note that when k increases, the maxima that appear are smaller. After $k = 430$, for all $k \leq k^*$, one can use $\sigma \approx 1.253475$ which appears for $k = 11504929$. If we look at all the γ_j^* , $j = 1, \dots, 6$, one has that from $k = 10^2$, 10^3 and 10^6 on, values of $\sigma = 1.7215$, 1.2944 and 1.1283 , respectively, are enough for all of them. Perhaps bounds of the form $|N_k - \gamma D_k| > c / (D_k \log(D_k) (\log(\log(D_k)))^\delta)$ with $\delta > 1$ and $c > 0$ not too small can also be found. This condition is also satisfied by a set of γ of full measure.

The previous items give strong evidences that the γ_j^* , $j = 1, \dots, 6$, behave as one should expect for a set of γ of full measure. However, to prove that they satisfy Khinchin and Lévy limits and Gauss-Kuzmin distribution seem to be not easy questions.

Finally we turn to the hidden HBA. As a first thing, we have checked in all the cases that no two consecutive best approximants are hidden and that, when one is hidden, next quotient is equal to 1, in agreement with the theorem. Furthermore it has been checked that this happens even when the denominators D_k are small. If the k -th best approximant is hidden one has that the probability to have a quotient, q_k , which is small (say, 1, 2, 3) is less than the theoretical probability $P(k)$ of the Gauss-Kuzmin law.

Next point will be to see how the hidden HBA are found on the average. To this end we concentrate again on $\pi - 3$ and proceed as follows. First we detect all the hidden HBA which appear up to the 10^7 -th best approximant. We have 2785810 of them. Then we consider blocks of 1000 consecutive BA, i.e., between 1 and 1000, between 1001 and 2000, etc, up to a total of 10000 blocks. In each block we look for how many hidden HBA are found. The minimum and maximum are 242 and 317, which appear only once, but the value 278 appears 438 times.

From these data one can construct the cumulative distribution function, CDF^* , of the hidden HBA which appear in blocks of 1000 consecutive BA. It turns out that the CDF^* is extremely close to the CDF of a normal law (see Fig. 5, left). One checks that the maximum of the differences in absolute value of both functions is small and this ensures that the sample passes the Kolmogorov-Smirnov test (see Fig. 5, right). The mean m and standard deviation s have been slightly tuned, with respect to the ones of the sample, to have a smaller maximal amplitude of the differences. Looking at all the γ_j^* , $j = 1, \dots, 6$, one has done similar computations up to the best approximant of order 4×10^6 (i.e., just 4000 blocks). The maxima of $|CDF^* - CDF|$ is, in all cases, less than 0.0068, still very good taking into account the reduction of the size of the sample. Similar values of m, s have been used in all cases.

Therefore it seems natural to formulate the following conjecture for systems giving rise to quasi-periodic splitting under assumptions similar to the ones in Sect. 4.

Conjecture 6.1. For a set of ratios of two frequencies of full measure, the distribution of the the hidden best approximant harmonics follows a normal law.

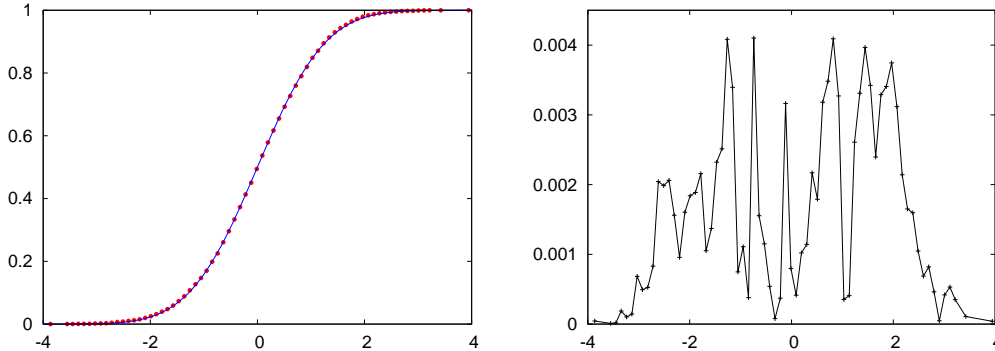


Figure 5: Left: Cumulative distribution function, CDF^* , of the hidden HBA for γ_1^* . If l is the number of hidden HBA in blocks of 1000 consecutive BA, the horizontal variable is $x = (l-m)/s$ where $m = 279.118$, $s = 9.604$. The experimental values CDF^* are plotted as red points. The curve in blue is the CDF of the normal law $N(0, 1)$. Right: Using the same horizontal variable as in the left part, the plot shows $|CDF^*(x) - CDF(x)|$. The maximum is ≈ 0.0041 .

7 Conclusions

The paper has clarified the existence of hidden HBA under suitable assumptions, which explains the results of numerical simulations. We have also done several computations using frequencies such that there is numerical evidence that they behave in a typical way. For the simple system that we have considered the numerical evidence supports that more than one fourth of the harmonics associated to best approximants are hidden.

The methodology can be applied to general problems, perhaps depending on several parameters. We hope that these ideas could be useful to identify the relevant near-resonances for the behavior of the splitting in concrete physical systems. This has, in turn, important consequences on the dynamics of the system.

One can ask many natural related questions. Among them we can mention:

Question 1. If we consider the variations of both first integrals G_1 and G_2 due to splitting, one can check that for some ranges of ν the splittings of both functions are close to be proportional: $\Delta\tilde{F}_2 \approx \alpha\Delta\tilde{F}_1$. Then $G_2 - \alpha G_1$ would act as a kind of additional first integral. Which is the effect on the local diffusive properties?

Question 2. In the case of three or more frequencies, which are the dominant harmonics in the splittings? How they evolve as a function of ν ? Which is the influence of the arithmetic properties of the involved frequencies?

Acknowledgments

This work has been supported by grants MTM2016-80117-P, MDM2014-0445 (Spain) and 2017-SGR-1374 (Catalonia). We are specially indebted to A. Delshams and M. Gonchenko for discussions on related topics. We also thank J. Timoneda for maintaining the computing facilities of the Dynamical Systems Group of the Universitat de Barcelona, that have been largely used in this work. We warmly thank the reviewers who suggested to add some references and to enlarge the Introduction, to improve the readability of the paper.

References

- [1] Barrabés, E., Ollé, M., Borondo, F., Farrelly, D., Mondelo, J. M.: Phase space structure of the hydrogen atom in a circularly polarized microwave field, *Physica D* **241**, 333-349 (2012).
- [2] Batut, C., Belabas, K., Bernardi, D., Cohen, H., and Olivier, M.: *Users' guide to PARI/GP*, <http://pari.math.u-bordeaux.fr/>
- [3] Delshams, A., Gonchenko, M., Gutiérrez, P.: Exponentially Small Lower Bounds for the Splitting of Separatrices to Whiskered Tori with Frequencies of Constant Type. *International Journal of Bifurcation and Chaos* **24**: 1440011 (2014), 12 pp.
- [4] Delshams, A., Gonchenko, M., Gutiérrez, P.: Continuation of the exponentially small transversality for the splitting of separatrices to a whiskered torus with silver ratio, *Regul. Chaotic Dyn.* **19**, 663-680 (2014).
- [5] Delshams, A., Gonchenko, M., Gutiérrez, P.: Exponentially small splitting of separatrices and transversality associated to whiskered tori with quadratic frequency ratio, *SIAM J. Appl. Dyn. Syst.* **15**, 981-1024 (2016).
- [6] Delshams, A., Gutiérrez, P.: Splitting potential and the Poincaré-Melnikov method for whiskered tori in Hamiltonian systems, *J. Nonlinear Sci.* **10**, 433-476 (2000).
- [7] Delshams, A., Gutiérrez, P.: Exponentially small splitting for whiskered tori in Hamiltonian systems: continuation of transverse homoclinic orbits, *Discrete Contin. Dyn. Syst.* **11**, 757-783 (2004).
- [8] Delshams, A., Gelfreich, V., Jorba, À., M.-Seara, T.: Exponentially small splitting of separatrices under fast quasiperiodic forcing, *Comm. Math. Phys.* **189**, 35-71 (1997).
- [9] Fontich, E., Simó, C., Vieiro, A.: Splitting of the separatrices after a Hamiltonian-Hopf bifurcation under periodic forcing. Preprint, 2018.
- [10] Khinchin, A. Ya.: *Continued Fractions*, The University of Chicago Press, Chicago, Ill.-London, 1964.
- [11] Kuzmin, R. O.: On a problem of Gauss, *Doklady Akad. Nauk. SSSR*, 375-380 (1928).
- [12] Lochak, P., Marco, J.-P., Sauzin, D. On the splitting of invariant manifolds in multidimensional near-integrable Hamiltonian systems, *Mem. Amer. Math. Soc.* 163 (2003), no 775, viii+145 pp.
- [13] Moser, J.: On invariant curves of area-preserving mappings of an annulus, *Nachr. Akad. Wiss. Göttingen Math.-Phys. Kl. II*, 1-20 (1962).
- [14] Moser, J.: *Stable and random motions in dynamical systems. With special emphasis on celestial mechanics*, Princeton University Press, 1973.
- [15] Ollé, M., Pacha, J. R.: Hopf bifurcation for the hydrogen atom in a circularly polarized microwave field, *Commun. Nonlinear Sci. Numer. Simulat.* **62**, 27-60 (2018).
- [16] Rudnev, M., Wiggins, S.: Existence of exponentially small separatrix splitting and homoclinic connections between whiskered tori in weakly hyperbolic near-integrable Hamiltonian systems, *Physica D* **114**, 3-90 (1998).

- [17] Rudnev, M., Wiggins, S.: On the dominant Fourier modes in the series associated with separatrix splitting for an a priori stable, three degrees-of-freedom Hamiltonian system, in *The Arnoldfest, Proceedings of a conference in Honour of V.I. Arnold for his Sixtieth Birthday*, E. Bierstone et al. eds., Fields Institute Communication Series **24**, AMS Publ., 1999, pp. 415-449.
- [18] Simó, C.: Averaging under fast quasiperiodic forcing. In I. Seimenis, editor, *Proceedings of the NATO-ARW Integrable and chaotic behavior in Hamiltonian Systems, Torun, Poland, 1993*, 13-34, Plenum Pub. Co., New York, 1994.
- [19] Simó, C., Valls, C.: A formal approximation of the splitting of separatrices in the classical Arnold's example of diffusion with two equal parameters, *Nonlinearity*, **14**, 1707-1760 (2001).